Synthesis, Characterization, and Photochemical/Photophysical Properties of Ruthenium(II) Complexes with Hexadentate Bipyridine and Phenanthroline Ligands

Ruth F. Beeston,*,† W. Stephen Aldridge,‡ Joseph A. Treadway,§ Michael C. Fitzgerald,|| Benjamin A. DeGraff,⊥ and Shannon E. Stitzel▽

Department of Chemistry, Davidson College, Davidson, North Carolina 28036

Received October 17, 1997

Three hexadentate, podand-type, polypyridyl ligands, $(5\text{-bpy-2C})_3\text{Bz}$, $(4\text{-bpy-2C-Ph})_3\text{Et}$, and $(4\text{-phen-2C-Ph})_3\text{Et}$, and their Ru(II) and Fe(II) complexes have been prepared. Reaction of these ligands with Fe(II) produces only the monometallic hemicage species, while monometallic, bimetallic, and polymetallic Ru(II) complexes are formed. These species are separable by column chromatography, and NMR and ESI mass spectrometry demonstrate that with each ligand the first band to elute corresponds to the monometallic species, $[\text{RuL}]^{2+}$. The ESI mass spectra show peaks for $[\text{RuL}]^{2+}$ and $[\text{RuL}](\text{PF}_6)^+$ with expected *m*/*z* values and isotope peak spacings. ^{1}H NMR spectroscopy shows that $[\text{Ru}(5\text{-bpy-2C})_3\text{Bz}]^{2+}$ is trigonally symmetric and contains a rigid methylene bridge between the capping group and the bipyridines. The excited-state lifetimes and emission quantum yields for the hemicage complexes, $[\text{Ru}(5\text{-bpy-2C})_3\text{Bz}]^{2+}$, $[\text{Ru}(4\text{-bpy-2C-Ph})_3\text{Et}]^{2+}$, and $[\text{Ru}(4\text{-phen-2C-Ph})_3\text{Et}]^{2+}$, are significantly enhanced (τ = 2800, 1470, and 3860 ns, and Φ_{em} = 0.271, 0.104, 0.202, respectively) relative to the model compounds and to the polymetallic complexes with the same ligand. An Arrhenius fit of temperature-dependent lifetime data for $[\text{Ru}(5\text{-bpy-2C})_3\text{Bz}]^{2+}$ indicates a high activation energy for crossover to the dd state (ΔE = 4960 cm^{-1}) as well as the existence of an additional pathway for deactivation via a "4th MLCT" state. Only after extensive photolysis of $[\text{Ru}(5\text{-bpy-2C})_3\text{Bz}]^{2+}$ is any decrease in emission intensity observed; this is accompanied by the formation of a bimetallic photoproduct, $[\text{Ru}_2\text{L}_2]^{4+}$, with a quantum yield of 7.4×10^{-6}. Quenching studies with a variety of quenchers show that the useful excited-state redox and energy-transfer properties characteristic of Ru(II) polypyridyls are retained, but with improved photoinertness and photophysical properties arising from the rigidity of the hemicage complex.

Introduction

The linking together of unidentate or bidentate ligands via suitable bridging groups, to produce cage-type coordination compounds, has been shown to be a viable approach to the design of complexes which are resistant to ligand dissociation.[1−3] Without changing the composition and symmetry of the first coordination sphere, replacement of "*n*" ligands with a suitably designed "*n*-dentate" ligand can have a dramatic effect on the thermodynamic and kinetic properties of the complex. This approach has been applied to the development of selective metal coordinating agents,[4] artificial sequestering agents,[5] inert complexes of labile metal ions,[6] stable oxidants and reductants for electron-transfer studies,[7] and photoinert complexes capable of performing useful light-induced functions.[8−16]

Within the last 10 years, the cage approach has been utilized in the design of transition metal tris(bipyridine) complexes with

† Davidson College.
‡ Present address: University of North Carolina, Chapel Hill, NC.
§ Present address: Affymax Research Institute, Palo Alto, CA.
|| Present address: Duke University, Durham, NC.
⊥ Present address: James Madison University, Harrisonburg, VA.
▽ Present address: Tufts University, Medford, MA.

(1) Balzani, V.; Sabbatini, N.; Scandola, F. *Chem. Rev.* **1986**, *86*, 319.
(2) Balzani, V. *Gazz. Chim. It.* **1989**, *119*, 311.
(3) Balzani, V. *Pure Appl. Chem.* **1990**, *62*, 1099.
(4) See for example: (a) Thompson, J. A.; Barr, M. E.; Ford, D. K.; Silks, L. A.; McCormick, J.; Smith, P. H. *Inorg. Chem.* **1996**, *35*, 2025. (b) Ghosh, P.; Gupta, S. S.; Bharadwaj, P. K. *J. Chem. Soc., Dalton Trans.* **1997**, 935. (c) Lehn, J.-M.; Montavon, F. *Helv. Chim. Acta* **1978**, *61*, 67.
(5) See for example: (a) Garrett, T. M.; McMurry, T. J.; Hosseini, M. W.; Reyes, Z. E.; Hahn, F. E.; Raymond, K. N. *J. Am. Chem. Soc.* **1991**, *113*, 2965. (b) Rodgers, S. J.; Lee, C.-W.; Ng, C. Y.; Raymond, K. N. *Inorg. Chem.* **1987**, *26*, 1622. (c) Motekaitis, R. J.; Sun, Y.; Martell, A. E. *Inorg. Chem.* **1991**, *30*, 1554.
(6) See for example: (a) Geue, R. J.; Hambley, T. W.; Harrowfield, J. M.; Sargeson, A. M.; Snow, M. R. *J. Am. Chem. Soc.* **1984**, *106*, 5478. (b) Creaser, I. I.; Geue, R. J.; Harrowfield, J. M.; Herlt, A. J.; Sargeson, A. M.; Snow, M. R.; Springborg, J. *J. Am. Chem. Soc.* **1982**, *104*, 6016. (c) Creaser, I. I.; Harrowfield, J. M.; Herlt, A. J.; Sargeson, A. M.; Springborg, J.; Geue, R. J.; Snow, M. R. *J. Am. Chem. Soc.* **1977**, *99*, 3181.
(7) See for example: (a) Mok, C.; Zanella, A. W.; Creutz, C.; Sutin, N. *Inorg. Chem.* **1984**, *23*, 2891. (b) Creaser, I. I.; Gahan, L. R.; Geue, R. J.; Launikonis, A.; Lay, P. A.; Lydon, J. D.; McCarthy, M. G.; Mau, A. W.-H.; Sargeson, A. M.; Sasse, W. H. F. *Inorg. Chem.* **1985**, *24*, 2671. (c) Lay, P. A.; Mau, A. W.-H.; Sasse, W. H. F.; Creaser, I. I.; Gahan, L. R.; Sargeson, A. M. *Inorg. Chem.* **1983**, *22*, 2347.
(8) See for example: (a) Ghosh, P.; Bharadwaj, P. K.; Mandal, S.; Ghosh, S. *J. Am. Chem. Soc.* **1996**, *118*, 1553. (b) Bodar-Houillon, F.; Marsura, A. *New. J. Chem.* **1996**, *20*, 1041. (c) Pina, F.; Mulazzani, Q. G.; Venturi, M.; Ciano, M.; Balzani, V. *Inorg. Chem.* **1985**, *24*, 848. (d) Sabbatini, N.; Perathoner, S.; Balzani, V.; Alpha, B.; Lehn, J.-M. In *Supramolecular Photochemistry*; Balzani, V., Ed., Reidel Publ. Co.: Dordrecht, Holland, 1987; p 187.
(9) Rodriguez-Ubis, J.-C.; Alpha, B.; Plancherel, D.; Lehn, J.-M. *Helv. Chim. Acta* **1984**, *67*, 2264.
(10) Sabbatini, N.; Mecati, A.; Guardigli, M.; Balzani, V.; Lehn, J.-M.; Zeissel, R.; Ungaro, R. *J. Lumin.* **1991**, *48−49*, 463.
(11) Grammenudi, S.; Vögtle, F. *Angew. Chem., Int. Ed. Engl.* **1986**, *25*, 1122.
(12) Belser, P.; De Cola, L.; von Zelewsky, A. *J. Chem. Soc., Chem. Commun.* **1988**, 1057.
(13) De Cola, L.; Barigelletti, F.; Balzani, V.; Belser, P.; von Zelewsky, A.; Vögtle, F.; Ebmeyer, F.; Grammenudi, S. *J. Am. Chem. Soc.* **1988**, *110*, 7210; **1989**, *111*, 4662.

S0020-1669(97)01322-0 CCC: $15.00
Published on Web 08/01/1998

Chart 1

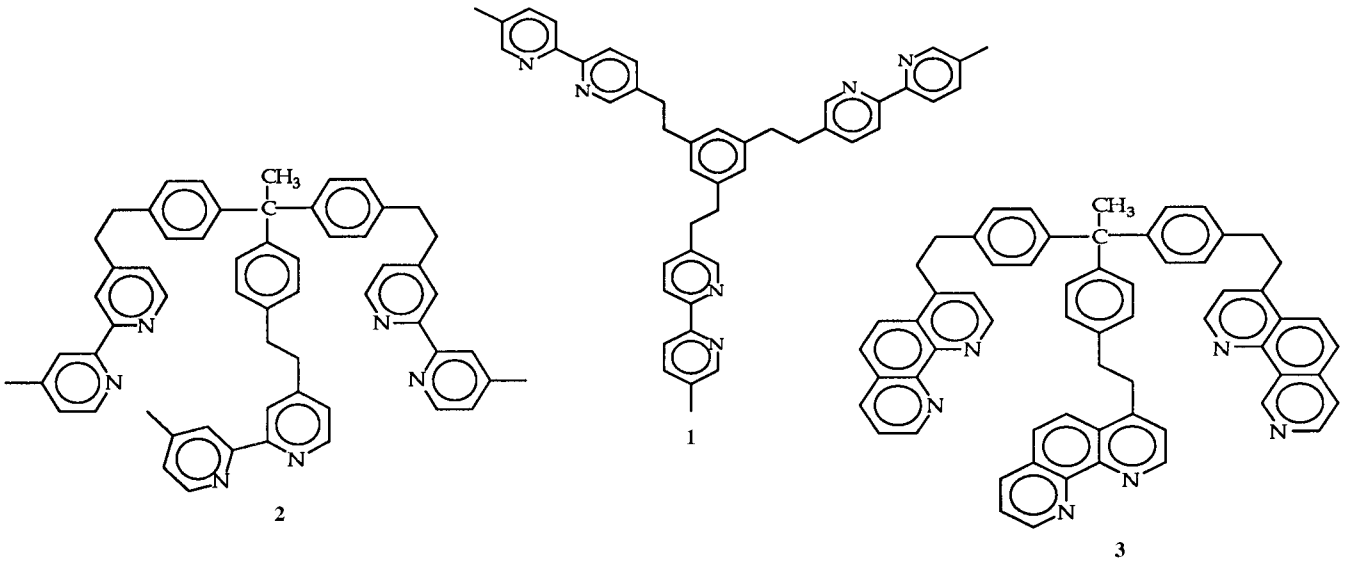

enhanced photophysical properties and which are resistant to photodecomposition.[9−16] Such complexes are of great interest, since they combine the features of thermal, electrochemical, and photosubstitutional inertness characteristic of cage complexes, with the useful photochemical, photophysical, and redox properties of metal polypyridine complexes.[17] Of particular interest are ruthenium(II) polypyridyl complexes, which exhibit metal-to-ligand charge-transfer (MLCT) excited states which can be highly luminescent, sufficiently long lived to participate in bimolecular reactions, and capable of acting as electron donors or acceptors or as energy donors. Such compounds have been widely studied in the past three decades due to their ability to act as sensitizers for light to chemical energy conversion.[18]

Along these research lines, we have prepared a series of trigonally symmetric, hexadentate polypyridyl ligands, whose structures are given in Chart 1 (**1**, (5-bpy-2C)$_3$Bz (previously referred to as (Mebpy)$_3$Bz);[14] **2**, (4-bpy-2C-Ph)$_3$Et; and **3**, (4-phen-2C-Ph)$_3$Et). These ligands are capable of encapsulating transition metal ions or acting as bridging ligands in polymetallic assemblies. We report here a detailed study of the structure and excited-state properties of ruthenium(II) complexes of ligands **1**, **2**, and **3**.

Previously reported cage-type polypyridyl complexes take a variety of forms, including closed cage complexes, or cryptates, in which the three bipyridyl ligands are capped on two opposite faces with tripodal bridging groups,[9−13] and hemicage, or podate complexes, in which a single capping group on one face connects the three bidentate ligands.[13−15] A photoinert ruthenium complex described as a "coronate", in which each of the three bipyridine ligands is tethered to the other two by crown ether linkages, has also been reported.[16] A novel linked bis-(terpyridine)ruthenium(II) catenane, in which the linking group contains a phenanthroline and is interlocked with another phenanthroline-containing ring, provides an additional example of a cage-type system.[19] In this complex, the two interlocked phenanthroline groups provide a tetradentate binding site for the formation of bimetallic complexes.

The first macrobicyclic ligands containing three bipyridine or phenanthroline groups were reported by Lehn et al.[9] Although lanthanide cryptates of these ligands have been prepared,[10] the cavity size is insufficient to allow an octahedral coordination environment around a transition metal ion. In 1986, the first macrocyclic tris(bipyridyl) ligand capable of forming closed-cage transition metal complexes was synthesized in 10 steps by Grammenudi and Vögtle.[11] An iron(II) complex of this ligand, which showed unusual inertness toward demetalation by EDTA and to acid decomposition, was reported. The ruthenium(II) analogue of this complex was prepared by Belser et al. via a template approach,[12] and this closed-cage ruthenium-(II) complex was found to exhibit ground-state properties which are very similar to those of $[Ru(bpy)_3]^{2+}$. However, the room temperature excited-state lifetime and the emission quantum yield of the cage complex are enhanced, while the quantum yield for ligand photodissociation is drastically reduced (by a factor of 10^4).[13] A hemicage version of this closed-cage ruthenium complex, in which only one capping group connects the three bipyridines, was also investigated. The absorption, emission, and photophysical properties of this complex were found to be intermediate between those of the parent complex, $[Ru(5,5'\text{-}(EtO_2C)_2bpy)_3]^{2+}$, and the closed-cage complex.[13] The drawbacks to these systems include the multistep syntheses, which require the Ru(II) ion to function as a template during the construction of the cage, and the amide linkages in the capping group, which may be reactive under certain conditions.

A hexadentate ligand constructed from three bis(diazine) groups and capable of forming hemicage complexes was recently reported by Duerr et al.[15] This ligand does not require a template synthesis, can easily accommodate a ruthenium(II) ion, and contains oligoethylene glycol spacers attached to a central benzene ring via ester linkages. The capping group in this compound is very large and flexible; enhancement in the luminescence lifetime is due to the electronic effects of the ethylene glycol substituents, not to a rigid cage environment. The photoinertness reported for the ruthenium complex of this

(14) Beeston, R. F.; Larson, S. L.; Fitzgerald, M. C. *Inorg. Chem.* **1989**, *28*, 4187.
(15) Dürr, H.; Schwarz, R.; Andreis, C.; Willner, I. *J. Am. Chem. Soc.* **1993**, *115*, 12362.
(16) Bossman, S.; Dürr, H. *New J. Chem.* **1992**, *16*, 769.
(17) Kalyanasundaram, K. *Photochemistry of Polypyridine and Porphyrin Complexes*; Academic Press: New York, 1992.
(18) Juris, A.; Balzani, V.; Barigelletti, F.; Campagna, S.; Belser, P.; von Zelewsky, A. *Coord. Chem. Rev.* **1988**, *84*, 85.
(19) Cardenas, D. J.; Gavina, P.; Sauvage, J.-P. *J. Am. Chem. Soc.* **1997**, *119*, 2656.

ligand was attributed to the cage effect, as well as to a stabilization of the MLCT level relative to the ligand field states upon replacement of bipyridine with bis(diazine). Again the presence of reactive functionalities in the linking groups is a drawback.

Another example of a photoinert, hemicage tris(bipyridyl)-ruthenium(II) complex (based on ligand **1**) was previously reported by our research group and was shown to exhibit an enhanced emission quantum yield and excited-state lifetime.[14] This is the first report of a polypyridyl cage-type complex of ruthenium(II) with completely unreactive tethers (methylene linkages to bridgehead benzene ring) rather than amide, ester, ether, or amine linkages. The ligand can be prepared by a relatively simple route, the formation of the complex does not rely on a template synthesis, and the approach is flexible enough to allow the synthesis of a variety of related hexadentate ligands and hemicage complexes.

The enhanced excited-state lifetimes and emission quantum yields, and diminished quantum yields for ligand photodissociation observed for closed cage and hemicage complexes are a result of the increased rigidity of the molecule imparted by the constraints of the bridging group(s). Because the three-dimensional structure of a cage complex reduces the freedom of motion of the ligand, processes requiring extensive nuclear displacement, such as radiationless decay via highly distorted structures and ligand dissociation or substitution reactions, are hindered in cage-type complexes.[2] Studies with complexes of ligands **1**, **2**, and **3**, which vary in terms of their rigidities (due to different size capping groups and the replacement of bipyridine with phenanthroline), were undertaken in order to more fully understand the nature of these structural effects on the electronic structure and excited-state dynamics of the polypyridyl Ru(II) chromophore. Representations of the structures of the hemicage complexes with ligands **1** and **2**, $[Ru(5\text{-bpy-}2C)_3Bz]^{2+}$ and $[Ru(4\text{-bpy-}2C\text{-}Ph)_3Et]^{2+}$, which show the positioning of the benzene or triphenylmethyl capping group above the octahedral $[Ru(bpy)_3]^{2+}$ center, are provided in Figure 1. The complex of ligand **3** has a structure similar to that of ligand **2**.

As previously reported,[14] the ground-state properties, such as absorption spectra and redox potentials, of $[Ru(5\text{-bpy-}2C)_3Bz]^{2+}$ are almost identical to those of the parent complex, tris(5,5′-dimethyl-2,2′-bipyridine)ruthenium(II), showing only slight shifts in λ_{max} and $E_{1/2}$. However, dramatic differences in the excited-state lifetime, the luminescence quantum yield, and the quantum yield for photodissociation were reported for this hemicage and parent pair. Since that report, improvements in our purification techniques have allowed us to reevaluate the properties of $[Ru(5\text{-bpy-}2C)_3Bz]^{2+}$ and to investigate the properties of ligand-linked polymetallic assemblies isolated from the same reaction mixture. In addition, the synthesis of ligands **2** and **3** and their Ru(II) hemicage complexes has allowed us to probe the effects of capping group, position of substitution, and replacement of bipyridine with phenanthroline.

Here we present the synthesis of the three hexadentate, podand ligands and their complexes with Ru(II) and Fe(II). The separation of mononuclear and ligand-bridged polymetallic complexes by cation exchange chromatography and the characterization of the individual species by NMR spectroscopy and electrospray ionization mass spectrometry (ESI-MS) are also described. The technique of ESI-MS has only recently been applied to the characterization of transition metal complex ions. Mass spectra of $[Ru(bpy)_3]^{2+}$ and $[Ru(phen)_3]^{2+}$ obtained by the electrospray ionization technique were first reported by Chait, et al. in 1990,[20] and more recently, the characterization of polynuclear complexes by ESI-MS has been reported.[21]

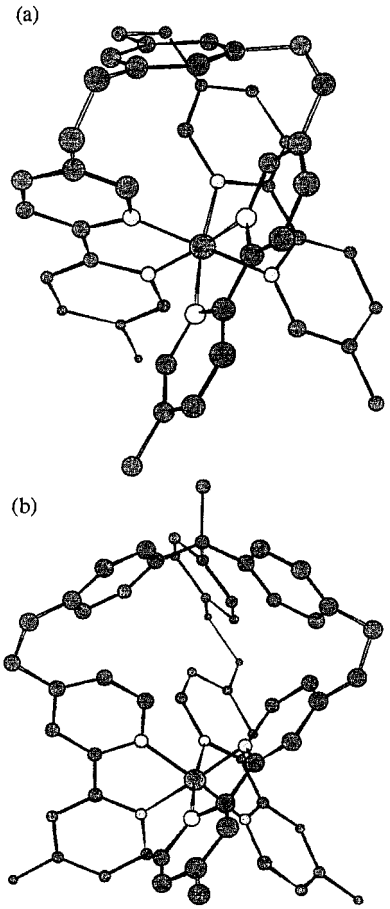

Figure 1. Representations of structures of hemicage complexes: (a) $[Ru(5\text{-bpy-}2C)_3Bz]^{2+}$ and (b) $[Ru(4\text{-bpy-}2C\text{-}Ph)_3Et]^{2+}$.

In this study we report on the spectroscopic properties, room-temperature excited-state lifetimes, and emission quantum yields of the ruthenium(II) complexes of $(5\text{-bpy-}2C)_3Bz$, $(4\text{-bpy-}2C\text{-}Ph)_3Et$, and $(4\text{-phen-}2C\text{-}Ph)_3Et$, as well as their corresponding parent complexes, which contain the bidentate ligands, 5,5′-dimethyl-2,2′-bipyridine (5,5′-dmb), 4,4′-dimethyl-2,2′-bipyridine (4,4′-dmb), or 4-methylphenanthroline (4-Mephen). A more detailed study of the photochemical and photophysical properties of $[Ru(5\text{-bpy-}2C)_3Bz]^{2+}$ is presented. This includes an investigation of the solvent and temperature dependence of the excited-state lifetime, stability toward photodissociation, and bimolecular quenching behavior.

Experimental Section

Materials. 5,5′-Dimethyl-2,2′-bipyridine (5,5′-dmb) was prepared by coupling 3-picoline in the presence of Pd^0 on charcoal[22] and was recrystallized from ethyl acetate. 4,4′-Dimethyl-2,2′-bipyridine (4,4′-dmb) and 4-methyl-1,10-phenanthroline (4-Mephen) were obtained from Reilley Tar and Chemical and GFS Chemicals, respectively, and

(20) Katta, V.; Chowdhury, S. K.; Chait, B. T. *J. Am. Chem. Soc.* **1990**, *112*, 5348.
(21) (a) Leize, E.; Van Dorsselaer, A.; Kramer, R.; Lehn, J.-M. *J. Chem. Soc., Chem. Commun.* **1993**, 990. (b) Hopfgartner, G.; Piguet, C.; Henion, J. D.; Williams, A. F. *Helv. Chim. Acta*, **1993**, *76*, 1759. (c) Arakawa, R.; Matsuo, T.; Ito, H.; Katakuse, I.; Nozaki, K.; Ohno, T.; Haga, M. *Org. Mass Spectrom.* **1994**, *29*, 289. (d) Ortmans, I.; Didier, P.; Mesmaeker, K.-D. *Inorg. Chem.* **1995**, *34*, 3695. (e) Arakawa, R.; Matsuo, T.; Nozaki, K.; Ohno, T.; Haga, M. *Inorg. Chem.* **1995**, *34*, 2464. (f) Bignozzi, C. A.; Bortolini, O.; Curcuruto, O.; Hamdan, M. *Inorg. Chim. Acta* **1995**, *223*, 113.

recrystallized from ethyl acetate. Diethyl ether and tetrahydrofuran (THF) were distilled over sodium and benzophenone just prior to use. Diisopropylamine was dried by passage through an oven dried alumina column. *n*-Butyllithium (1−2.5 M in hexane) was standardized by titration with *sec*-butanol prior to use. $Ru(DMSO)_4Cl_2$ was prepared by literature methods.[23] Chromatographic silica gel (type A60, 200−425 mesh) was obtained from Fisher Scientific. SP Sephadex C-25 was obtained from Sigma Chemical Co. Silica gel TLC uniplates were from Analtech. All other reagents and solvents were from Aldrich, Fisher, or Kodak and used without further purification. Elemental analyses were performed by Midwest Microlab.

Synthesis of Capping Agents. 1,3,5-Tris(bromomethyl)benzene. In a 500 mL round-bottom flask equipped with a water-cooled condenser, *N*-bromosuccinimide (NBS, 27.8 g, 0.156 mol), mesitylene (7.5 mL, 0.054 mol), and 2,2′-azobis(2-methylpropionitrile) (AIBN, 50 mg) were combined with 200 mL of methyl formate. This mixture was irradiated with a GE 250 W reflector infrared heat lamp placed 6 in. from the flask, causing the methyl formate to reflux. During approximately 45 min of irradiation, the NBS dissolved, giving a light orange solution. Irradiation was continued for an additional 30 min. The reaction was followed by TLC on silica gel (20% dichloromethane in cyclohexane; R_f for dibromide = 0.55; R_f for tribromide = 0.39). The methyl formate was removed by rotary evaporation, leaving a thick yellow oil that crystallized upon sitting overnight. To this residue, 20 mL of water was added and the mixture was extracted with 2 × 50 mL dichloromethane. The dichloromethane layers were combined, washed with 2 × 50 mL of 2% aqueous sodium carbonate solution and 2 × 50 mL water, and dried over sodium sulfate. The dichloromethane was removed by rotary evaporation, leaving a pale yellow, waxy solid, which was recrystallized three times from hot cyclohexane. The resulting white solid (4.8 g, 26%) was shown by NMR to be 96% tribromide and 4% dibromide. Anal. Calcd for $C_9H_9Br_3$: C, 30.29; H, 2.54; Br, 67.17. Found: C, 30.23; H, 2.57; Br, 66.91. ^{1}H NMR (in $CDCl_3$): δ 7.36 (s, 3H), 4.43 (s, 6H).

1,1,1-Tris(4-bromomethylphenyl)ethane, $(BrCH_2Ph)_3Et$. This compound was prepared in four steps using a modification of literature procedures.[24] Tris(4-methylphenyl)methanol was prepared via Grignard reaction of 4-tolylmagnesium bromide (0.225 mol) and ethyl-4-methylbenzoate (0.096 mol) in diethyl ether.[24a] The reaction mixture was poured onto a mixture of 6 M sulfuric acid and ice, and the product was extracted with ether and isolated by rotary evaporation. The resulting oil was converted to chlorotris(4-methylphenyl)methane by refluxing in acetyl chloride (60 mL).[24b] The product precipitated upon cooling and was isolated by filtration and dried, yielding 20 g (70%). Chlorotris(4-methylphenyl)methane (19 mmol) in dry toluene was treated with methylmagnesium iodide (45 mmol) in dry ether.[24b] The reaction mixture was heated at reflux then cooled, water was slowly added, and the product was isolated by extraction with ether. Rotary evaporation yielded 4.9 g (87%) of 1,1,1-tris(4-methylphenyl)ethane ($(CH_3Ph)_3Et$).

Bromination was carried out by combining $(CH_3Ph)_3Et$ (2.06 g, 6.87 mmol), NBS (3.68 g, 20.7 mmol), AIBN (30 mg), and 185 mL of methyl formate in a round-bottom flask equipped with a reflux condensor. The mixture was stirred and irradiated with a 250 W heat lamp for 90 min, causing the solid to dissolve and the solution to reflux. The mixture was stirred for an additional 30 min without irradiation. A white solid formed and was isolated by filtration. To the solid, 40 mL of water was added, and the mixture was extracted with dichloromethane (2 × 40 mL). The organic layers were combined and evaporated, leaving a white solid which contained a mixture of the dibrominated and tribrominated products. Recrystallization was accomplished by dissolving the solid in a minimum of dichloromethane, adding an equal volume of cyclohexane, and allowing the solution to sit in an ice bath for 1 h. The resulting precipitate was filtered and determined by NMR to be 95% pure $(BrCH_2Ph)_3Et$. A yield of 1.2 g (32%) was obtained. ^{1}H NMR ($CDCl_3$): δ 7.31 (d, 6H), 7.08 (d, 6H), 4.50 (s, 6H), 2.08 (s, 3H).

Synthesis of Hexadentate Ligands. 1,3,5-Tris((5′-methyl-2,2′-bipyridin-5-yl)ethyl)benzene, $(5\text{-bpy-}2C)_3Bz$ (1). All glassware was oven dried overnight and cooled in a desiccator before use. A 500 mL three-neck round-bottom flask containing 20 mL of freshly distilled THF was flushed with nitrogen and immersed in a dry ice/acetone bath. Dry diisopropylamine (3.2 mL, 22 mmol) and *n*-butyllithium in hexane (14.0 mL, 1.46 M, 20.4 mmol) were added via syringe. The LDA solution was stirred for 10 min, and a solution of 5,5′-dmb (5.00 g, 27.2 mmol) in 200 mL THF was added via cannula. The resulting dark black reaction mixture was stirred at −78 °C for 90 min. A solution of 1,3,5-tris(bromomethyl)benzene (2.17 g, 6.08 mmol) in 40 mL THF was added via cannula. The flask was removed from the ice bath and the black solution was stirred for 90 min. Upon addition of 20 mL of water, a color change to yellow was noted. The THF was removed by rotary evaporation, and an additional 50 mL of water was added. The mixture was extracted with 3 × 50 mL dichloromethane. The combined organic extracts were washed with 2 × 25 mL water, dried with anhydrous sodium sulfate, and evaporated to dryness, leaving a solid yellow residue. The product was isolated by column chromatography on silica gel (1:9 THF/CH_2Cl_2 was used to elute excess 5,5′-dimethylbipyridine; $(5\text{-bpy-}2C)_3Bz$ was collected with 2:8 THF/CH_2Cl_2). Fractions containing $(5\text{-bpy-}2C)_3Bz$ were combined and evaporated, and the solid residue was recrystallized from ethanol, yielding 2.15 g (53%). Anal. Calcd for $C_{45}H_{42}N_6$: C, 81.05; H, 6.35; N, 12.60. Found: C, 80.98; H, 6.44; N, 12.42. ^{1}H NMR ($CDCl_3$): δ 8.49 (s, 3H), 8.39 (s, 3H), 8.22 (m, 6H), 7.60 (m, 3H), 7.53 (m, 3H), 6.78 (s, 3H), 2.90 (s, br, 12H), 2.40 (s, 9H).

1,1,1-Tris(4-((4′-methyl-2,2′-bipyridin-4-yl)ethyl)phenyl)ethane, $(4\text{-bpy-}2C\text{-}Ph)_3Et$ (2). THF (10 mL) and diisopropylamine (0.56 mL, 4.1 mmol) were combined in a three-neck flask at −78 °C under nitrogen. *n*-Butyllithium (2.4 mL, 1.73 M, 4.1 mmol) was added via syringe, and after 15 min a solution of 4,4′-dimethyl-2,2′-bipyridine (1.5 g, 8.2 mmol) in 50 mL of THF was added via cannula. The reaction mixture was stirred for 80 min prior to addition of $(BrCH_2Ph)_3Et$ (0.550 g, 1.02 mmol) in 15 mL of THF. The ice bath was removed, and the solution was stirred overnight. Water (25 mL) was added, and the product was extracted with dichloromethane. The organic extracts were evaporated to dryness, and the remaining solid was applied to a silica gel chromatography column. A mobile phase of 1:7 THF/CH_2Cl_2 was used to elute the excess 4,4′-dmb, and 3:2:15 THF/ethanol/CH_2Cl_2 was used to isolate the $(4\text{-bpy-}2C\text{-}Ph)_3Et$. Fractions containing the desired product were combined, evaporated, and the resulting solid recrystallized from ethanol. Anal. Calcd for $C_{59}H_{54}N_6$: C, 83.65; H, 6.43; N, 9.92. Found: C, 83.23; H, 6.38; N, 9.72. ^{1}H NMR ($CDCl_3$): δ 8.58 (m, 6H), 8.27, (m, 6H), 7.17 (m, 6H), 7.08 (d, 6H), 7.00 (d, 6H), 3.02 (s, br, 12H), 2.44 (s, 9H), 2.16 (s, 3H).

1,1,1-Tris(4-((1,10-phenathrolin-4-yl)ethyl)phenyl)ethane, $(4\text{-phen-}2C\text{-}Ph)_3Et$ (3). *n*-Butyllithium (3.3 mL, 1.04 M, 3.4 mmol) was added via syringe to a solution of THF (10 mL) and diisopropylamine (0.50 mL, 3.6 mmol) at −78 °C under nitrogen. The LDA solution was stirred for 15 min, and to this was added via cannula a solution of 4-methylphenanthroline (1.17 g, 6.03 mmol) dissolved in 40 mL of THF. The dark solution was stirred continuously under nitrogen for 1 h. A solution of $(BrCH_2Ph)_3Et$ (0.540 g, 1.00 mmol) in 35 mL of THF was added via cannula, and the reaction flask was removed from the ice bath. The reaction mixture was stirred overnight, and 25 mL of water was added. The product and excess 4-Mephen were extracted with 2 × 20 mL of dichloromethane. The dichloromethane layers were combined, washed with 3 × 40 mL of water, dried over anhydrous sodium sulfate, and evaporated. The residue was applied to a silica gel column, and 1:1 THF/CH_2Cl_2 was used as the first mobile phase to elute 4-Mephen. $(4\text{-Phen-}2C\text{-}Ph)_3Et$ was then isolated with 4:2:5 THF/methanol/CH_2Cl_2. ^{1}H NMR ($CDCl_3$): δ 9.16 (d, 3H), 8.95 (d, 3H), 8.27 (d, 3H), 8.00 (d, 3H), 7.78 (d, 3H), 7.61 (m, 3H), 7.32 (d, 3H), 6.99 (d, 6H), 6.90 (d, 6H), 3.43 (t, 6H), 3.10 (t, 6H), 2.15 (s, 3H).

Synthesis of Ruthenium(II) Complexes. $[Ru(5\text{-bpy-}2C)_3Bz](PF_6)_2$. Ethanol (300 mL, 95%) containing $(5\text{-bpy-}2C)_3Bz$ (67 mg, 0.10

(22) Weinheimer, C.; Choi, Y.; Caldwell, T.; Gresham, P.; Olmsted, J., III. *J. Photochem. Photobiol. A* **1994**, *78*, 119.
(23) Evans, I. P.; Spencer, A.; Wilkinson, G. *J. Chem. Soc., Dalton Trans.* **1973**, 204.
(24) (a) Hohner, G.; Vögtle, F. *Chem. Ber.* **1977**, *110*, 3052. (b) Dung, B.; Vögtle, F. *J. Incl. Phenom.* **1988**, *6*, 429.

mmol) was heated to reflux under nitrogen. A solution of $Ru(DMSO)_4Cl_2$ (49 mg, 0.10 mmol) in 20 mL of 95% ethanol was added, and reflux was continued for 6 h. The solvent was removed by rotary evaporation, leaving a red-orange solid. From this, several ruthenium species were isolated by column chromatography on a SP Sephadex C-25 support. A light yellow impurity was removed with 5:3 aqueous NaCl (0.05 M)/acetone. The hemicage species, $[Ru(5\text{-bpy-}2C)_3Bz]^{2+}$ (BAND A1) was eluted with 5:3 aqueous NaCl (0.1 M)/acetone. Two additional bands were collected with mobile phases of 5:3 aqueous NaCl (0.15 M)/acetone (BAND A2) and 5:3 aqueous NaCl (0.2 M)/acetone (BAND A3), respectively. Acetone was removed from the fractions by evaporation, and the complexes were precipitated by addition of saturated aqueous ammonium hexafluorophosphate. A typical yield of 50 mg of $[Ru(5\text{-bpy-}2C)_3Bz](PF_6)_2$ was obtained from BAND A1 (47%). Alternatively, if the chloride salt was needed, the complex was isolated by evaporation of the appropriate fraction to dryness, addition of ethanol to the residue, and filtration to remove NaCl.

$[Ru(4\text{-bpy-}2C\text{-}Ph)_3Et](PF_6)_2$. $Ru(DMSO)_4Cl_2$ (30 mg, 0.062 mmol) was added to a refluxing solution of $(4\text{-bpy-}2C\text{-}Ph)_3Et$ (54 mg, 0.062 mmol) in 300 mL of 95% ethanol under nitrogen. Reflux was continued for 5 h, and the solvent was removed by rotary evaporation, yielding a dark orange oil. The oil was dissolved in a minimum of 5:3 aqueous NaCl (0.05 M)/acetone and applied to an SP Sephadex C-25 column. Two orange bands were collected as the NaCl concentration in the aqueous portion of the mobile phase was maintained at 0.05 M (BAND B1) and then increased to 0.10 M (BAND B2). Acetone was removed by evaporation, and the complexes were isolated by the addition of NH_4PF_6 (aq).

$[Ru(4\text{-phen-}2C\text{-}Ph)_3Et](PF_6)_2$. $Ru(DMSO)_4Cl_2$ (20 mg, 0.042 mmol) was added to a refluxing solution of $(4\text{-phen-}2C\text{-}Ph)_3Et$ (30 mg, 0.042 mmol) in 800 mL of 95% ethanol under nitrogen. Reflux was continued for 7.5 h, resulting in a gradual color change to orange. The solvent was removed by rotary evaporation. The dark orange residue was dissolved in a minimum of 5:3 aqueous NaCl (0.05 M)/acetone and applied to a SP Sephadex C-25 column. Three orange bands were collected as the NaCl concentration in the aqueous portion of the mobile phase was maintained at 0.05 M (BAND C1), then increased to 0.10 M (BAND C2), then increased to 0.20 M (BAND C3). Acetone was removed by evaporation, and the complexes were isolated by the addition of NH_4PF_6 (aq).

Synthesis of Iron(II) Complexes. $[Fe(5\text{-bpy-}2C)_3Bz]Cl_2$. A solution of ferrous ammonium sulfate (78 mg, 0.20 mmol) in 20 mL of ethanol/water was added to a refluxing solution of $(5\text{-bpy-}2C)_3Bz$ (130 mg, 0.20 mmol) in 95% ethanol (580 mL). The red solution was refluxed under nitrogen for 5 h. The solvent was removed by rotary evaporation, leaving a dark red solid. The iron hemicage complex was isolated from the residue by chromatography on SP-Sephadex C-25, using 5:3 aqueous NaCl (0.05 M, then 0.10 M)/acetone. The complex eluted as a single dark red band, with a small amount of a red impurity remaining at the origin. The eluent was evaporated to dryness, and the remaining solid was dissolved in absolute ethanol, which was then filtered to remove NaCl and evaporated.

$[Fe(4\text{-bpy-}2C\text{-}Ph)_3Et]Cl_2$. A solution of ferrous ammonium sulfate (5.2 mg, 0.013 mmol) in 5 mL of water was added to a refluxing solution of $(4\text{-bpy-}2C\text{-}Ph)_3Et$ (11.3 mg, 0.0133 mmol) in 95% ethanol (300 mL). The red solution was refluxed under nitrogen for 5 h. The solvent was removed by rotary evaporation. The iron hemicage complex was isolated from the residue by chromatography on SP-Sephadex C-25, using 5:3 aqueous NaCl (0.05 M, then 0.10 M)/acetone. A single red band eluted from the column. The eluent was evaporated to dryness, the remaining solid was dissolved in absolute ethanol, and the ethanol solution was filtered to remove NaCl.

Instrumental Methods. NMR Spectroscopy. NMR spectra were recorded on a Bruker AC-300 FT NMR, using $CDCl_3$ (for ligands and precursors) or CD_3CN (for metal complexes) as solvent.

Electrospray Ionization Mass Spectrometry (ESI-MS). Mass spectra were acquired on a Sciex API-III quadrupole electrospray mass spectrometer. Samples were analyzed in 1:1 water/acetonitrile at concentrations of approximately 10 μM. Samples were electrosprayed from a small capillary (100 μm i.d.) using a flow rate of 5 μL/min. Typically, mild interface conditions (low orifice potentials of 40−50 V) were used to minimize the disruption of the Ru−ligand complexes under study.

Visible Absorption Spectroscopy. Visible absorption spectra of the complexes in acetonitrile were recorded on a Perkin-Elmer Lambda 6 spectrophotometer.

Photophysical Measurements. Room-temperature emission spectra (500−900 nm) and emission quantum yields were obtained with a SPEX Fluorolog-2 emission spectrometer equipped with a 450 W xenon lamp and a Hamamatsu 666-01 PMT. Spectra were corrected for variations in lamp intensity by monitoring the emission intensity of Rhodamine-B and for PMT response using a NIST calibrated standard lamp (Optronics Laboratories, Inc., model 220 M) controlled with a precision current source at 6.50 A (Optronics Laboratories, Inc., model 65). Samples were dissolved in acetonitrile (or other solvent as specified) in 1 cm path length quartz cells and deaerated (40 min) with oxygen-scrubbed Ar. Emission quantum yields (Φ_{em}) were measured relative to $[Ru(bpy)_3](PF_6)_2$ in acetonitrile ($\Phi'_{em} = 0.062$)[25] and were calculated using the equation

$$\Phi_{em} = \Phi'_{em}\left(\frac{I_{sample}}{I_{std}}\right)\left(\frac{A_{std}}{A_{sample}}\right)\left(\frac{\eta^2_{sample}}{\eta^2_{std}}\right)$$

where I_{sample} and I_{std} are the integrated emission intensities, A_{sample} and A_{std} are the absorbances at the excitation wavelenth, and η_{sample} and η_{std} are the refractive indices of the solvents for the sample and $[Ru(bpy)_3](PF_6)_2$, respectively.

Excited-state lifetimes were measured for argon-deaerated acetonitrile solutions (optically dilute, $A < 0.15$) at room temperature, using a nitrogen laser (PRA LN1000) to pump a dye laser (PRA LN102) using Coumarin 460 dye. The emitted light was observed at right angles to the excitation beam with a MacPherson 272 scanning monochromator set at the emission maximum of each complex. The emission was monitored with a Hamamatsu R446 PMT-LeCroy 7200 digitizing oscilloscope combination interfaced to a PC. The average of 200 traces was fit to an exponential model ($I_t = I_0\ e^{-kt}$) using a Levenburg−Marquardt minimization routine. Lifetime measurements in other solvents were obtained using degassed, optically dilute solutions of the PF_6^- or Cl^- salt of $[Ru(5\text{-bpy-}2C)_3Bz]^{2+}$. Temperature-dependent lifetime data were acquired for a solution of $[Ru(5\text{-bpy-}2C)_3Bz](PF_6)_2$ dissolved in 4:1 ethanol/methanol in an NMR tube. The solution was freeze−pump−thaw degassed (4×), and the tube was flame-sealed. The tube was mounted in an Oxford cryostat (liquid nitrogen cooled, helium carrier gas) containing a copper heat bath, which was heated with an Oxford Instruments 3120 temperature controller. Temperature was measured via a thermocouple placed at the sample tube, using an Omega HH-51 digital thermometer. Measurements were conducted on the samples when thermal equilibration had been maintained for 10 min.

Photochemical Measurements. The quantum yield for photosubstitution was measured for an acetonitrile solution of $[Ru(5\text{-bpy-}2C)_3Bz](PF_6)_2$ (prepared to give an absorbance of 1.0 at the irradiation wavelength in a 1 cm cell) containing a 1000-fold excess of tetrabutylammonium chloride. The sample was sparged with oxygen-scrubbed argon for 1 h, and was irradiated with a 75 W Xe lamp (XBO 75W/2) powered by a high-precision constant source. Light was passed through a monochromator and focused to a point 1 cm into the sample cell. The sample was stirred continuously and thermostated at 25 °C. The sample cell had a 12 cm path length to ensure that all light was absorbed, and the cell was equipped with a sidearm leading to a 1 cm cuvette. At regular intervals the cell was removed from the light beam, shaken, and tilted to allow solution to flow into cuvette for emission intensity measurement. Emission intensity (I) was monitored as a function of time, and the fraction dimerized at time, t, (X_t) was calculated using the emission quantum yields of the hemicage complex (Φ) and the dimer (Φ_{dimer}) (see Results) as follows:

(25) Caspar, J. K.; Kober, E. M.; Sullivan, B. P.; Meyer, T. J. *J. Am. Chem. Soc.* **1982**, *104*, 630.

$$X_t = \left(1 - \frac{I_t}{I_0}\right)\left(\frac{\Phi}{\Phi - \Phi_{\text{dimer}}}\right)$$

A plot of X_t vs t was prepared, and the quantum yield for dimerization was calculated from the slope of this plot, the initial moles of the hemicage complex, and the intensity of the light source (as determined from the rate of photodissociation of $[Ru(bpy)_3]^{2+}$).

The photoproduct was detected by cation-exchange HPLC on a Brownlee CX-300 Prep 10 column. Mobile phase A consisted of 3:1 aqueous phosphate buffer (pH 7)/acetonitrile; mobile phase B consisted of A plus 200 mM KBr. Elution proceeded as follows: 0−5 min, 100% A; 5−30 min, 0−75% B; 30−45 min, 75−0% B). Elutions were controlled with a Rainin Dynamax SD-300 solvent delivery system equipped with 25 mL/min pump heads. Detection from 250 to 700 nm (2 nm spacing) was accomplished via a Shimadzu SPD-M10AV diode array UV−visible spectrometer fitted with a 4.5 mm path length flow cell.

Quenching constants were determined from Stern−Volmer plots of τ^0/τ vs quencher concentration ($\tau^0/\tau = 1 + k_q\tau^0[Q]$). Linear plots were obtained, and k_q values were calculated from the slopes obtained by linear regression. In a typical experiment, a series of acetonitrile solutions approximately 1.5×10^{-5} M in chromophore ($[Ru(5,5'\text{-dmb})_3](PF_6)_2$ or $[Ru(5\text{-bpy-2C})_3Bz](PF_6)_2$), 0.1 M in $NaClO_4$, and containing various concentrations of quencher (0−4 mM) were prepared. Solutions were degassed with acetonitrile-saturated N_2 for 15 min prior to lifetime measurement. For the oxygen quenching studies, air saturated and O_2 saturated samples were prepared by sparging with the appropriate gas for 15 min at 25 °C. Samples were irradiated with a pulsed nitrogen laser (Laser Science VSL-337) with a 3 ns pulse width. The 337 nm laser line was isolated by a Corion 337 nm interference filter. For samples in which the quencher was also a strong absorber at 337 nm (phenothiazine) the nitrogen laser was fitted with a broad band dye module using Coumarin 2. Standard 90° viewing was used with the emission light first passing through a saturated $NaNO_2$ solution and a sharp cutoff long-pass filter and then to a R928 PMT. The decay was captured on a Hewlett-Packard 5402A digital oscilloscope, and the digitized trace was transferred to a PC for data analysis. At least 100 traces were averaged for each determination. In all cases, a single exponential was adequate for fitting the decay curve.

Results and Discussion

Synthesis of Hemicage Complexes. The formation of the ruthenium(II) hemicage complexes with ligands **1**, **2**, and **3** was accompanied by formation of polymetallic complexes which were eluted from the cation exchange column as the NaCl concentration in the mobile phase was increased. An orange band which was not mobile even with eluents of high ionic strength remained at the top of the column. The competing formation of linked polynuclear complexes occurred even under reaction conditions of high dilution and was more evident when using the ligands capped with 1,1,1-triphenylethane (**2** and **3**) than with ligand **1**. Molecular models show that with the ligands $(4\text{-bpy-2C-Ph})_3Et$ and $(4\text{-phen-2C-Ph})_3Et$, two bipyridine-(phenanthroline) "arms" can bind to the ruthenium ion in such a way that the third bipyridine(phenanthroline) cannot reach the remaining binding site to form a mononuclear hemicage species. The resulting Ru complex has an available binding site and a free polypyridyl group, and can combine with one or more similar species to form $[Ru_nL_n]^{2n+}$ type complexes. In contrast, $(5\text{-bpy-2C})_3Bz$ has a benzene cap that can invert to allow coordination of the third bipyridine following complexation of two bipyridine arms. Although linked polymetallic complexes still formed with this ligand, a greater yield of the hemicage complex was isolated.

Interestingly, reaction of $(5\text{-bpy-2C})_3Bz$ and $(4\text{-bpy-2C-Ph})_3Et$ with iron(II) produced almost exclusively the mononuclear hemicage complex, $[FeL]^{2+}$, as evidenced by the presence of a single band on the cation exchange column. Since iron(II) complexes are more thermally labile than analogous ruthenium-(II) complexes, the bipyridyl groups bind and dissociate numerous times, allowing the most thermodynamically stable arrangement to finally be achieved. Once the hemicage species is formed, dissociation of a ligand arm is likely to be followed by "reannealing", since the dissociated bipyridine is kept in close proximity.

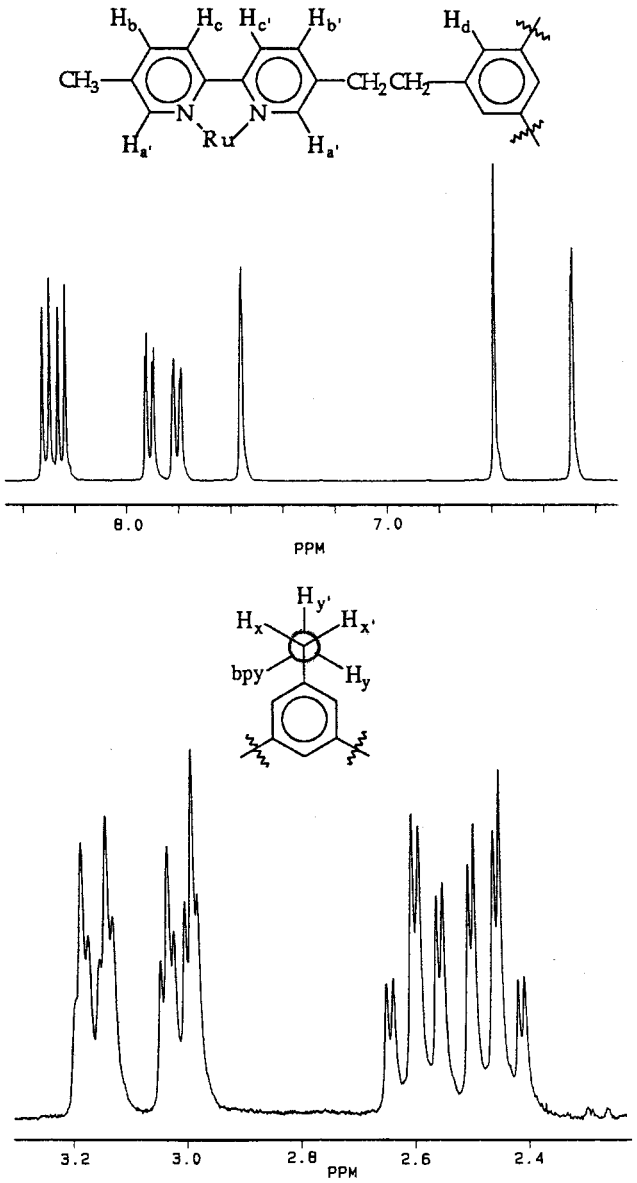

Figure 2. ^1H NMR spectrum of $[Ru(5\text{-bpy-2C})_3Bz](PF_6)_2$ (BAND A1) in CD_3CN. Top trace, aromatic protons; lower trace, methylene protons. Insets show structure and proton designations for NMR assignments given in text.

NMR Spectra of $[Ru(5\text{-bpy-2C})_3Bz]^{2+}$, $[Fe(5\text{-bpy-2C})_3Bz]^{2+}$, and $[Fe(4\text{-bpy-2C-Ph})_3Et]^{2+}$. The aromatic and methylene regions of the NMR spectrum of $[Ru(5\text{-bpy-2C})_3Bz]^{2+}$ (BAND A1) are shown in Figure 2, and insets on this figure show the structures and proton designations for the aromatic and methylene groups. The aromatic region shows 7 signals, as expected for the trigonally symmetric hemicage structure. The singlet at 6.59 ppm was attributed to H_d, the three equivalent protons on the phenyl cap (these appear at 6.8 ppm for uncomplexed $(5\text{-bpy-2C})_3Bz$). The peaks at 7.55 and 6.28 ppm were assigned to the pyridyl protons adjacent to the nitrogens, H_a and $H_{a'}$, respectively. In the NMR spectrum of uncomplexed (5-bpy-

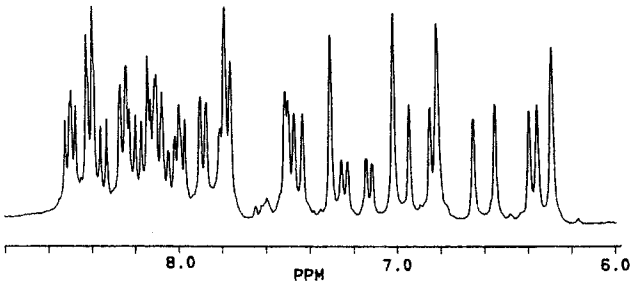

Figure 3. Aromatic region of ^{1}H NMR spectrum of Ru(II) complex with (5-bpy-2C)$_3$Bz (BAND A3).

2C)$_3$Bz, signals for these protons were observed at 8.4−8.5 ppm. The chemical shifts of H_a and $H_{a'}$ exhibit the greatest dependence on complexation. The large difference in the chemical shifts of these two protons is due to the positioning of $H_{a'}$ under the capping phenyl group in the complex, which causes a large upfield shift for this proton. The pair of doublets with chemical shift >8.2 ppm were attributed to pyridyl protons adjacent to the bipyridine ring junction (H_c and $H_{c'}$), which show coupling only to H_b and $H_{b'}$. The remaining pair of doublets (7.8 and 7.9 ppm), arising from H_b and $H_{b'}$, show additional coupling to H_a and $H_{a'}$.

The NMR spectrum of the methylene region of [Ru(5-bpy-2C)$_3$Bz]$^{2+}$, shown in the lower trace in Figure 2, has four unique signals with many coupling interactions, indicating that the -CH_2-CH_2- linkages are equivalent and conformationally "locked" within the hemicage complex. The splitting patterns are consistent with a staggered conformation, as depicted in the inset in Figure 2. In this conformation protons H_x and H_y each experience geminal coupling (to $H_{x'}$ and $H_{y'}$, respectively) with an expected coupling constant (J) of 12−18 Hz, as well as two vicinal coupling interactions to protons with dihedral angles of about 60° (expected $J = 2-4$ Hz) and 180° (expected $J = 8-14$ Hz).[26] The two triplets of doublets (2.4−2.7 ppm) were thereby assigned to H_x and H_y, with the following coupling constants: $J_{xx'} = J_{yy'} = J_{xy} = 13$ Hz; $J_{xy'} = J_{x'y} = 3$ Hz. The two doublets of triplets (3.0−3.2 ppm) could therefore be attributed to $H_{x'}$ and $H_{y'}$, which each experience geminal coupling (13 Hz) as well as coupling to two vicinal protons, both with a dihedral angle of 60° in the staggered conformation ($J_{xy'} = J_{x'y} = J_{x'y'} = 3$ Hz). In the NMR spectrum of the uncomplexed hexadentate ligand, the methylene protons were observed as a single broad signal at 2.9 ppm.

The spectrum shown in Figure 2 is consistent with a hemicage structure for BAND A1 of the Ru complex. Figure 3 shows the aromatic region of the NMR spectrum of BAND A3 isolated from the reaction of Ru(DMSO)$_4$Cl$_2$ and (5-bpy-2C)$_3$Bz. It indicates the presence of at least 20 nonequivalent protons on the bipyridine and phenyl capping groups of this complex. Clearly this species does not have a symmetrical hemicage structure; the complicated spectrum is consistent with a polynuclear ligand-bridged species in which the three bipyridines on a single ruthenium are not in equivalent environments.

With the ligand, (5-bpy-2C)$_3$Bz, the NMR spectrum of the hemicage complex of Fe(II) is nearly identical to that of [Ru(5-bpy-2C)$_3$Bz]$^{2+}$ shown in Figure 2. The NMR spectrum of [Fe(5-bpy-2C)$_3$Bz]$^{2+}$ (Supporting Information, Figure S1) exhibits identical splitting patterns as well as chemical shifts that agree to within 0.1 ppm for comparable protons. The exceptions

(26) Silverstein, R. M.; Bassler, G. C.; Morrill, T. C. *Spectrometric Identification of Organic Compounds*, 5th ed.; Wiley: New York, 1991; pp 196−197.

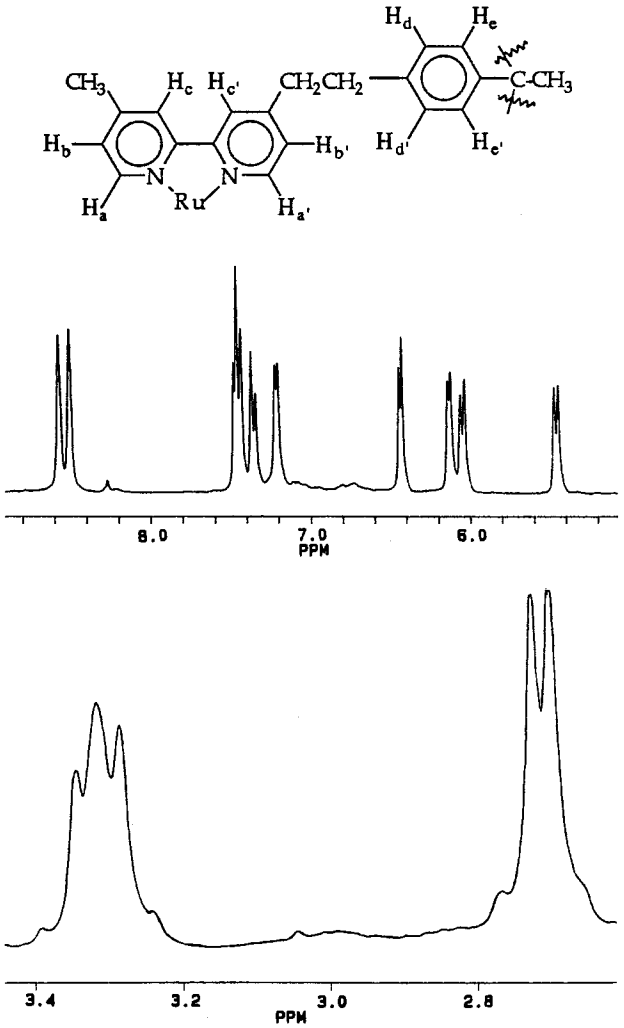

Figure 4. NMR spectrum of [Fe(4-bpy-2C-Ph)$_3$Et](PF$_6$)$_2$ in CD_3CN. Top trace, aromatic protons; lower trace, methylene protons. Inset shows structure and proton designations for NMR assignments given in text.

to this are the signals for H_a and $H_{a'}$, which are shifted upfield by about 0.4 ppm when Ru(II) is replaced with Fe(II). For the ligand, (4-bpy-2C-Ph)$_3$Et, the NMR spectrum was recorded for the Fe(II) complex only, since the reaction of the hexadentate ligand with this metal produced exclusively the hemicage complex, while only small quantities of [Ru(4-bpy-2C-Ph)$_3$Et]$^{2+}$ could be isolated.

The NMR spectrum of [Fe(4-bpy-2C-Ph)$_3$Et]$^{2+}$ is shown in Figure 4, along with a structure indicating the proton designations for the aromatic protons. The presence of two broad peaks for the methylene protons implies that hemicage complexes with this capping group are more flexible than those with the smaller 1,3,5-trisubstituted benzene cap. Rotation around the C−C bond of the methylene bridge is apparently less restricted than in the hemicage complexes of (5-bpy-2C)$_3$Bz. The aromatic region of the spectrum shows the expected number of signals for the 10 unique aromatic protons on the bipyridine and capping phenyl groups. Of these 10 peaks, the only singlets at 8.58 and 8.51 ppm could be assigned to H_c and $H_{c'}$. (These exhibit similar chemical shifts to the corresponding protons in the parent complex, [Fe(4,4′-dmb)$_3$]$^{2+}$). The most unusual feature of the NMR spectrum of [Fe(4-bpy-2C-Ph)$_3$Et]$^{2+}$ is the appearance of four doublets between 5.4 and 6.5 ppm. No aromatic proton signals in the parent complex or unbound ligand spectra appear this far upfield. Molecular models show that in the hemicage complex, $H_{a'}$ and $H_{b'}$ are positioned under the bridging phenyl

group, while $H_{d'}$, and $H_{e'}$ (the bridging phenyl protons which point toward the metal center) are positioned over the pyridine ring to which the bridging group is attached. Therefore these protons are expected to be more highly shielded, and most likely give rise to the doublets from 5.4 to 6.5 ppm. The doublets at 6.1 and 6.4 ppm exhibit a small coupling constant (5 Hz) characteristic of the bipyridyl protons, $H_{a'}$ and $H_{b'}$. Doublets at 5.4 and 6.0 ppm ($J = 8$ Hz) could therefore be assigned to $H_{d'}$ and $H_{e'}$. The remaining signals between 7.2 and 7.5 ppm correspond to the protons H_a and H_b (the pyridyl protons on the ring not affected by the capping group, which exhibit a chemical shift of 7.2 in the parent complex), and to H_d and H_e (the bridging phenyl protons which point away from the metal center, which appear as doublets at 7.0 and 7.1 ppm in the spectrum of unbound (4-bpy-2C-Ph)$_3$Et). This spectrum is consistent with a hemicage structure in which all three bipyridine groups and all three "arms" of the capping group are equivalent.

Electrospray Ionization Mass Spectrometry (ESI-MS). For ligands **1**, **2**, and **3** one can envision, in addition to the hemicage complex containing one ruthenium encapsulated by one ligand, a series of ligand-linked polynuclear complexes constructed of "*n*" ruthenium(II) ions and "*n*" ligands. For example, a dimer in which each of two Ru(II) ions is bound to two hexadentate ligands (one via two bipyridine "arms" and one via one bipyridine "arm") is possible. ESI-MS was used to determine the charges and formulas of the various ruthenium species which were separated chromatographically, and to confirm the hemicage structure of the complexes of interest. The electrospray ionization method provides a gentle means of producing gas phase ions directly from solution. Metal complexes are characterized by an examination of the *m*/*z* ratio of the ions produced and of the isotopic patterns obtained by increasing the resolution of the spectrum. The spacing between the isotope peaks within the cluster ($\Delta m/z$) depends on the ion charge ($\Delta m/z = 1.0$ for a +1 ion, 0.5 for a +2 ion, etc.).

Ruthenium complexes of ligands **1**, **2**, and **3** were studied by ESI-MS in water/acetonitrile solutions as PF_6^- salts. At relatively low orifice potentials (40−50 V), peaks were observed for ions of the type $[Ru_nL_n]^{2n+}$ with varying numbers of counterions attached. ESI-MS was first used to investigate the three complexes of ruthenium with (5-bpy-2C)$_3$Bz which were isolated by ion exchange chromatography on Sephadex. BAND A1, which eluted at the lowest eluent ionic strength, was shown by NMR spectroscopy to be the mononuclear hemicage species, $[RuL]^{2+}$ (L = $C_{45}H_{42}N_6$, mass = 666 daltons; Ru = ^{102}Ru). The low-resolution ESI mass spectrum of BAND A1 is shown in Figure 5a; the two expected peaks at *m*/*z* 384 and 913 for $[RuL]^{2+}$ and $[RuL](PF_6)^+$, respectively, are present. Each of these peaks is actually a cluster of peaks due to the presence of seven naturally occurring ruthenium isotopes. Figure 5b and c shows the spectra of the two peaks obtained at enhanced resolution. Consistent with the mononuclear hemicage structure, the peak at *m*/*z* 384 is a cluster of isotope peaks separated by 0.5 *m*/*z* units, while the peak at *m*/*z* 913 shows the expected $\Delta m/z$ for a +1 ion. Furthermore, the experimental isotope profiles were in excellent agreement with the theoretical isotope distributions expected for the mononuclear species, $[RuL]^{2+}$ and $[RuL](PF_6)^+$. The ESI mass spectrum of BAND A1 did not change significantly as the orifice potential was increased to 100 V.

It is important to note that peaks at *m*/*z* 384 and 913 are also expected for polymetallic species $[Ru_nL_n]^{2n+}$ and $[Ru_nL_n](PF_6)_n^{n+}$, respectively. However, the ions producing these peaks would be more highly charged, and therefore the isotope peaks would be more closely spaced. Additional peaks at *m*/*z* ratios other than 384 and 913 would be present as well. The ESI mass spectrum of BAND A3, recorded at an orifice potential of 50 V, is presented in Figure 6a. For a dinuclear species, four peaks would be expected at *m*/*z* 384 ($[Ru_2L_2]^{4+}$), 560 ($[Ru_2L_2](PF_6)^{3+}$), 913 ($[Ru_2L_2](PF_6)_2^{2+}$), and 1971 ($[Ru_2L_2](PF_6)_3^{+}$). The presence of these four peaks, together with the isotopic patterns of the peaks at *m*/*z* 913 ($\Delta m/z = 0.5$) and *m*/*z* 1971 ($\Delta m/z = 1.0$), as shown in Figure 6b and c, are consistent with BAND A3 being a bimetallic complex. Good agreement was observed between the experimental and theoretical isotope distributions for $[Ru_2L_2](PF_6)_n^{4-n}$ species.

The ESI mass spectrum recorded for BAND A2 is very similar to that shown for BAND A3 in Figure 6a. However, the isotope patterns produced at high resolution do not match the theoretical spectra. In particular, the cluster of isotope peaks at *m*/*z* 913 shows the expected $\Delta m/z$ of 0.5, but alternating peaks are enhanced, suggesting the presence of both $[Ru_2L_2](PF_6)_2^{2+}$ and $[RuL](PF_6)^+$ in the electrospray. It was therefore concluded that BAND A2 may be a mixture of complexes or a species which decomposes in the electrospray to give mono- and bimetallic ions.

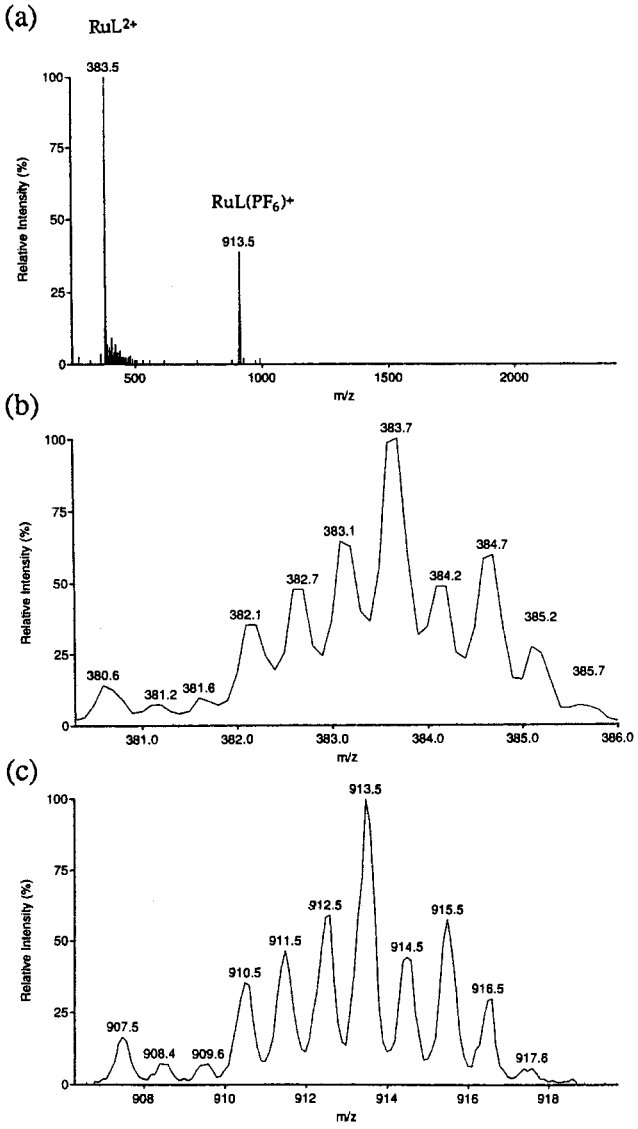

Figure 5. ESI mass spectra of Ru(II) complex with L = (5-bpy-2C)$_3$Bz, BAND A1; (a) low resolution; (b) high resolution of RuL^{2+}, $\Delta m/z = 0.5$; (c) high resolution of $RuL(PF_6)^+$, $\Delta m/z = 1.0$.

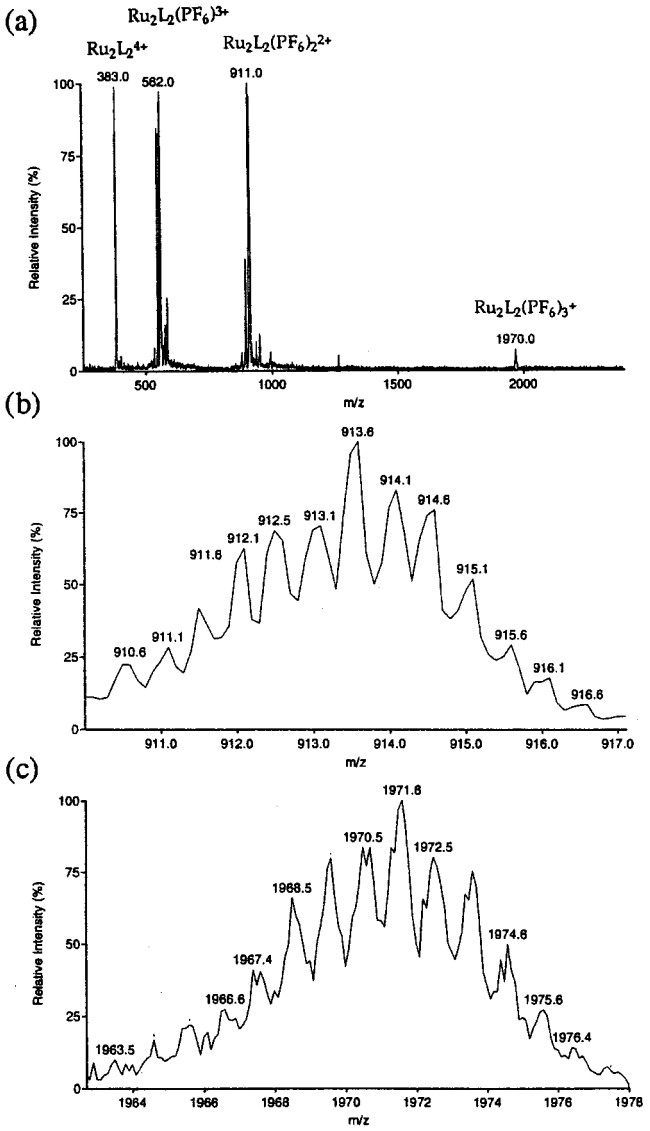

Figure 6. ESI mass spectra of Ru(II) complex with L = (5-bpy-2C)$_3$Bz, BAND A3; (a) low resolution; (b) high resolution of $Ru_2L_2(PF_6)_2^{2+}$, $\Delta m/z = 0.5$; (c) high resolution of $Ru_2L_2(PF_6)_3^{+}$, $\Delta m/z = 1.0$.

For Ru complexes of (4-bpy-2C-Ph)$_3$Et ($C_{59}H_{54}N_6$, mass = 846 daltons) and (4-phen-2C-Ph)$_3$Et ($C_{62}H_{48}N_6$, mass = 876 daltons), the first bands to be isolated from the Sephadex cation exchange column (BANDS B1 and C1) were studied by ESI-MS. The hemicage complex, $[Ru(4\text{-bpy-2C-Ph})_3Et]^{2+}$, would be expected to give peaks at m/z 474 ($\Delta m/z = 0.5$) for $[RuL]^{2+}$ and m/z 1093 ($\Delta m/z = 1.0$) for $[RuL](PF_6)^{+}$. For $[Ru(4\text{-phen-2C-Ph})_3Et]^{2+}$, corresponding peaks are expected at m/z 489 and 1123 daltons. The spectra (Supporting Information Figures S2 and S3) show peaks at the expected masses. The corresponding enhanced resolution spectra show that the isotopic separations are consistent with a mononuclear structure for these complexes.

Photophysical Properties. Table 1 is a summary of the absorption and room-temperature emission properties of the ruthenium(II) complexes of (5-bpy-2C)$_3$Bz, (4-bpy-2C-Ph)$_3$Et, and (4-phen-2C-Ph)$_3$Et. Data are included for the various bands isolated by column chromatography on the Sephadex resin. In each case, BAND 1 represents the mononuclear, hemicage complex, as confirmed by ESI-MS and/or NMR spectroscopy. As described previously, BAND 2 and BAND 3 samples likely correspond to polynuclear species (or mixtures of complexes). For comparison, values are provided for $[Ru(bpy)_3]^{2+}$ [25,27] and for the model complexes, $[Ru(5,5'\text{-dmb})_3]^{2+}$, $[Ru(4,4'\text{-dmb})_3]^{2+}$, and $[Ru(4\text{-Mephen})_3]^{2+}$. These parent species have the same ligand and methyl substitution pattern as the related hemicage species but lack the capping group. By comparing the photophysical properties of the ruthenium hemicage species to those of the appropriate parent species, it is possible to distinguish between the effects of caging and effects due to ligand type and substitution pattern.

Table 1. Absorption and Photophysical Properties of Ru(II) Complexes with Bidentate and Hexadentate Polypyridyl Ligands

	λ_{max} (nm)			
complex[a]	absorption	emission[b]	Φ_{em}[c]	τ (ns)[d]
$[Ru(bpy)_3]^{2+}$	452	621	0.062[25]	1100[27]
$[Ru(5,5'\text{-dmb})_3]^{2+}$	444	607	0.036	500
$[Ru(5\text{-bpy-2C})_3Bz]^{2+}$				
BAND A1	450	598	0.271	2800
BAND A2	446	605	0.022	*e*
BAND A3	447	606	0.044	570
$[Ru(4,4'\text{-dmb})_3]^{2+}$	452	636	0.079	810
$[Ru(4\text{-bpy-2C-Ph})_3Et]^{2+}$				
BAND B1	461	628	0.104	1470
BAND B2	458	632	0.063	*e*
$[Ru(4\text{-Mephen})_3]^{2+}$	446	606	0.045	590
$[Ru(4\text{-phen-2C-Ph})_3Et]^{2+}$				
BAND C1	450	600	0.202	3860
BAND C2	447	606	0.049	*e*
BAND C3	448	606	0.050	*e*

[a] All measurements were made in degassed solutions containing the PF_6^- salt of the complex in acetonitrile at 25 °C. [b] Corrected emission spectrum, λ_{ex} = 450 nm. [c] Measured relative to $[Ru(bpy)_3](PF_6)_2$ in acetonitrile (estimated uncertainty in quantum yields: ±20%, estimated precision and error of reported quantum yields relative to one another: ±5%). [d] Measured by laser flash photolysis following excitation at 460 nm (estimated uncertainty ±5%). [e] Multiexponential decay.

The wavelength of maximum absorption of each hemicage complex (BAND 1) is red shifted 4−9 nm compared to the corresponding model complex. However, emission λ_{max} values are 6−9 nm blue-shifted for the hemicage species. Assuming similar reorganizational parameters, the decrease in absorption energy and the increase in emission energy imply that the hemicage complexes in the MLCT excited state are less distorted relative to the ground state than are the model complexes in the MLCT state. The absorption and emission spectra of BAND 2 and BAND 3 samples are similar to those of the parent complexes or are intermediate between parent and hemicage spectra.

Emission quantum yields (Φ_{em}) in acetonitrile at room temperature are specified in Table 1. The quantum yields for the hemicage complexes are considerably larger than those of the parent complexes. A dramatic increase (a factor of 7.5 relative to $[Ru(5,5'\text{-dmb})_3]^{2+}$) was observed for $[Ru(5\text{-bpy-2C})_3Bz]^{2+}$, the most rigid of the hemicage complexes. The quantum yield of the more flexible complex, $[Ru(4\text{-bpy-2C-Ph})_3Et]^{2+}$, was determined to be 1.3 times that of the corresponding model complex, $[Ru(4,4'\text{-dmb})_3]^{2+}$. With the phenanthroline ligand, a 4-fold increase in Φ_{em} was observed for the hemicage complex relative to the parent complex, $[Ru(4\text{-Mephen})_3]^{2+}$. Interestingly, Φ_{em} for the bimetallic complex (BAND A3) was found to be similar to that of the parent complex, $[Ru(5,5'\text{-dmb})_3]^{2+}$; emission quantum yields for other BAND 2 and BAND 3 samples were also in agreement with the Φ_{em} values of the corresponding model complexes. These

(27) Juris, A.; Balzani, V.; Belser, P.; von Zelewsky, A. *Helv. Chim. Acta* **1981**, *64*, 2175.

results indicate that the rigid hemicage structure, and not the ligand itself, is responsible for the observed increases in Φ_{em}.

Encapsulation of Ru(II) by hexadentate ligands results in greatly increased room-temperature excited-state lifetimes (Table 1). A lifetime of 2800 ns (5.6 times that of the parent complex) was observed for $[Ru(5\text{-bpy-}2C)_3Bz]^{2+}$, making it among the longest lifetimes reported for tris(bipyridyl) complexes of Ru(II). An even longer excited-state lifetime, 3860 ns, was observed for $[Ru(4\text{-phen-}2C\text{-}Ph)_3Et]^{2+}$; this represents a 6.5-fold increase over the parent complex. Significantly, the lifetime of this phenanthroline hemicage complex is over twice as long as that of the bipyridine analogue, $[Ru(4\text{-bpy-}2C\text{-}Ph)_3Et]^{2+}$, which has the same capping group and substitution pattern. An opposite trend was observed with the parent complexes. In most cases, BAND 2 and BAND 3 samples exhibited multiexponential decay kinetics, and lifetimes are not reported for these species. The exception is BAND A3 from the $[Ru(5\text{-bpy-}2C)_3Bz]^{2+}$ reaction. This species, as described previously, appears to have a dinuclear structure, $[Ru_2((5\text{-bpy-}2C)_3Bz)_2]^{4+}$; it exhibited single-exponential decay kinetics and a lifetime comparable to that of the parent complex.

Several factors should contribute to the enhanced excited-state lifetimes of $[Ru(5\text{-bpy-}2C)_3Bz]^{2+}$, $[Ru(4\text{-bpy-}2C\text{-}Ph)_3Et]^{2+}$, and $[Ru(4\text{-phen-}2C\text{-}Ph)_3Et]^{2+}$. It is generally accepted that the excited-state lifetime of a polypyridyl ruthenium complex is governed by the rates of several deactivation pathways, including vibrational deactivation and thermal population of metal centered dd states of configuration $d\pi^5 d\sigma^{*1}$. When the ligands are covalently attached to a capping group, extensive excited-state distortion is hindered, and this decreases the rate of vibrational deactivation. Similar behavior has been observed in other constrained systems.[28] Consistent with this is the fact that the lifetime of $[Ru(5\text{-bpy-}2C)_3Bz]^{2+}$, which is known to be the more rigid of the two bipyridine hemicage complexes, is enhanced to a greater extent than that of $[Ru(4\text{-bpy-}2C\text{-}Ph)_3Et]^{2+}$. It is also possible that a decrease in the rate of thermal population of the dd excited states accompanies hemicaging. To quantify this effect on the excited-state dynamics of the hemicage species, the temperature dependence of the excited-state lifetime of $[Ru(5\text{-bpy-}2C)_3Bz]^{2+}$ was investigated.

In general, the observed rate constant of excited-state deactivation, k, is described by eq 1, where k_r and k_{nr} are the radiative and nonradiative rates:

$$1/\tau = k = k_{nr} + k_r \tag{1}$$

Usually for ruthenium(II) polypyridyl complexes, k_r is a minor contributor to the lifetime. This is not the case, however, for the hemicage system, due to unusually small radiationless decay rates. The radiative rate constant is expected to be relatively invariant over the temperature range of interest. The nonradiative rate can be expressed as

$$k_{nr} = k'_{nr} + k_{dd} \tag{2}$$

where k'_{nr} is the rate of vibrational deactivation by medium frequency (e.g. skeletal stretching modes on bipyridine) and low frequency (e.g. metal−ligand stretching and solvent modes) vibrations, and k_{dd} is the rate of deactivation via thermal population of dd or $^3(d\pi \rightarrow d\sigma^*)$ excited states. For complexes in which MLCT state deactivation occurs predominantly through the dd states and vibrational deactivation of the lowest manifold of MLCT states, the temperature dependence of the lifetime can generally be fit to the kinetic expression given in eq 3:[29]

$$k = \frac{k_0 + k_1 \exp(-\Delta E_1/k_B T)}{1 + \exp(-\Delta E_1/k_B T)} \tag{3}$$

where k_0 is the temperature-independent rate constant for deactivation of the MLCT state, ΔE_1 is the energy barrier for crossover from the MLCT state to the dd state, and k_1 is the rate constant of barrier crossing. While this expression adequately fits the temperature-dependent lifetime data for $[Ru(bpy)_3]^{2+}$ in fluid solution, evidence for the existence of an additional decay channel via thermal population of a higher energy MLCT state has been obtained for some complexes.[29] This "fourth" MLCT state plays an important role in the temperature dependence of the lifetime for Ru(II) complexes in rigid matrixes,[30] for osmium(II) polypyridyl complexes,[29,31] and for certain mixed ligand complexes in which the acceptor ligand has low π^* energy and/or is highly rigid.[32] In all of these cases, the MLCT to dd activation is inhibited in some way.

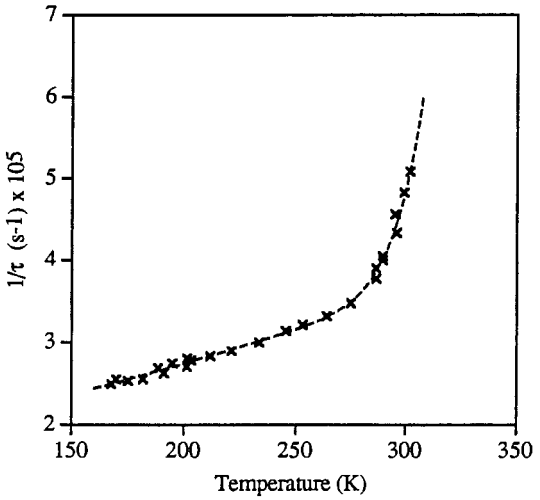

Figure 7. Temperature dependence of excited-state lifetime of $[Ru(5\text{-bpy-}2C)_3Bz](PF_6)_2$ in 4:1 ethanol/methanol (×, experimental data point; - - -, theoretical curve fit).

Excited-state lifetimes were measured for $[Ru(5\text{-bpy-}2C)_3Bz]^{2+}$ over the temperature range 167−302 K. Figure 7 shows a plot of decay rate ($1/\tau$, s^{-1}) vs temperature. Equation 3 did not provide an adequate fit for these data, and therefore the data were fit to a three-state model, as shown in eq 4:[29]

$$k = \frac{k_0 + k_1 \exp(-\Delta E_1/k_B T) + k_2 \exp(-\Delta E_2/k_B T)}{1 + \exp(-\Delta E_1/k_B T) + \exp(-\Delta E_2/k_B T)} \tag{4}$$

A Levenburg−Marquardt fitting routine was used to obtain the parameters k_0, k_1, k_2, ΔE_1, and ΔE_2 (where ΔE_1, and ΔE_2 represent the activation energies for crossover from the ^{3}MLCT state to the dd state and the higher energy MLCT state,

(28) Treadway, J. A.; Loeb, B.; Lopez, R.; Anderson, P. A.; Keene, F. R.; Meyer, T. J. *Inorg. Chem.* **1996**, *35*, 2242 and references therein.

(29) Lumpkin, R. S.; Kober, E. M.; Worl, L. A.; Murtaza, Z.; Meyer, T. J. *J. Phys. Chem.* **1990**, *94*, 239.

(30) (a) Allsopp, S. R.; Cox, A.; Kemp, T. J.; Reed, W. J. *J. Chem. Soc., Faraday Trans. 1* **1978**, *74*, 1275. (b) Maruszewski, K.; Strommen, D. P.; Kincaid, J. R. *J. Am. Chem. Soc.* **1993**, *115*, 8345.

(31) Allsopp, S. R.; Cox, A.; Kemp, T. J.; Reed, W. J.; Carassiti, V.; Traverso, O. *J. Chem. Soc., Faraday Trans. 1* **1979**, *75*, 353.

(32) For example: (a) Wacholtz, W. F.; Auerbach, R. A.; Schmehl, R. H. *Inorg. Chem.* **1986**, *25*, 227. (b) Barigelletti, F.; Juris, A.; Balzani, V.; Belser, P.; Von Zelewsky, A. *J. Phys. Chem.* **1987**, *91*, 1095.

Table 2. Kinetic Decay Parameters Obtained by Temperature-Dependent Lifetime Measurements

complex	k_0 (s^{-1})	k_1 (s^{-1})	ΔE_1 (cm^{-1})	k_2 (s^{-1})	ΔE_2 (cm^{-1})
$[Ru(bpy)_3]^{2+}$ [a]	5.6×10^5	5.8×10^{13}	3800		
$[Ru(5\text{-bpy-}2C)_3Bz]^{2+}$ [b]	2.1×10^5	3.5×10^{15}	4960	1.2×10^6	360

[a] From ref 33, temperature range 240−300 K in acetonitrile. [b] Temperature range 168−302 in 4:1 ethanol/methanol, estimated error on ΔE_1, ± 100 cm^{-1}.

Table 3. Solvent Dependence of Emission Properties of $[Ru(5\text{-bpy-}2C)_3Bz]^{2+}$ at 25 °C

solvent	λ_{max} (nm)	Φ_{em}	τ (ns)	k_r (s^{-1})	k_{nr} (s^{-1})
dichloromethane	584	0.36	2550	1.4×10^5	2.5×10^5
acetonitrile	598	0.27	2800	0.97×10^5	2.6×10^5
tetrahydrofuran	608	0.32	2640	1.2×10^5	2.6×10^5

respectively). The calculated parameters for the hemicage complex, $[Ru(5\text{-bpy-}2C)_3Bz]^{2+}$, are given in Table 2, along with previously reported values[33] for $[Ru(bpy)_3]^{2+}$ for comparison, and the theoretical curve fit to the data is shown in Figure 7. As expected based on increased rigidity, k_0 for the hemicage complex is somewhat smaller than for $[Ru(bpy)_3]^{2+}$. Significantly, the activation barrier for crossover to the dd state (ΔE_1) is more than 1000 cm^{-1} larger for $[Ru(5\text{-bpy-}2C)_3Bz]^{2+}$ than for $[Ru(bpy)_3]^{2+}$, but this state is still significant in the deactivation of the excited state at room temperature due to the large value for k_1. The results also point to the existence of an additional MLCT state, with an activation barrier (ΔE_2) of 360 cm^{-1} and a decay rate constant (k_2) of 1.2×10^6 s^{-1} (within the ranges established for higher lying MLCT excited states by Lumpkin et al.[29]).

The emission maximum, quantum yield, and room-temperature lifetime of $[Ru(5\text{-bpy-}2C)_3Bz]^{2+}$ were measured in several solvents of varying polarity, and the results are summarized in Table 3. The complexes were highly luminescent in all solvents, with the longest lifetime measured in acetonitrile. Values for the decay rates, k_r (Φ/τ) and k_{nr} ($1/\tau - k_r$), are also reported. The k_r values are typical for complexes of this type; however, k_{nr} values are unusually small. The slow rates of radiationless decay can be attributed to two factors, the rigidity imparted by the cage structure and the relative inaccessibility of the dd state, which lies at significantly higher energy in the hemicage complex. The results presented in Table 3 indicate that while the emission energy, quantum yield, and lifetime are somewhat solvent dependent, k_{nr} does not vary with solvent. Contrary to what is expected, it is the variation in radiative rate with solvent that seems to control the effect of solvent on the lifetime. Perhaps the weak dependence of k_{nr} on E_0 is an effect of the rigid nature of the complex, or the energy gap effects might be effectively canceled by dd state population differences, so that k_{nr} is practically constant in these three solvents. A more detailed analysis of the solvent and temperature effects of this and other hemicage systems is in progress.

Photochemistry of $[Ru(5\text{-bpy-}2C)_3Bz]^{2+}$. Photochemical reactivity of $[Ru(5\text{-bpy-}2C)_3Bz]^{2+}$ was compared to that of $[Ru(bpy)_3]^{2+}$, which has a quantum yield for photosubstitution of 0.029 in acetonitrile containing 2 mM tetrabutylammonium chloride.[34] Previously we reported that no photoinduced ligand loss (as evidenced by no observed decrease in absorbance at 450 nm) occurred for $[Ru(5\text{-bpy-}2C)_3Bz]^{2+}$ under these conditions.[14] However, this study revealed that, while absorbance at 450 did not change upon irradiation in these conditions, the emission intensity slowly decreased relative to a thermal blank.

Table 4. Rate Constants for the Quenching of $[Ru(5\text{-bpy-}2C)_3Bz](PF_6)_2$ and Its Model Complex by a Variety of Quenchers

	quenching rate constants, k_q (M^{-1} s^{-1})[a]	
quencher	$[Ru(5,5'\text{-dmb})_3]^{2+}$	$[Ru(5\text{-bpy-}2C)_3Bz]^{2+}$
oxygen	4.9×10^9	5.1×10^9
$[Fe(phen)_3]^{2+}$	7.2×10^8	9.9×10^8
methyl viologen	3.1×10^9	3.4×10^9
phenothiazine	1.7×10^9	3.6×10^9
4-aminoveratrole	3.6×10^8	8.5×10^8

[a] Rate constants measured in deaerated (except for O_2 quenching) acetonitrile, 0.1 M in $NaClO_4$ at 25 °C.

After irradiation for more than 1 day, HPLC analysis revealed the presence of a photoproduct with a retention time (t_R) of 27.4 min (t_R for the reactant, $[Ru(5\text{-bpy-}2C)_3Bz]^{2+}$, was 19.0 min). The retention time and absorbance spectrum of the photoproduct were determined to be the same as those of the complex present in BAND A3 (t_R = 27.1 min), which appears on the basis of ESI-MS to be the dimer, $[Ru_2((5\text{-bpy-}2C)_3Bz)_2]^{4+}$. This dimer exhibits a lower emission quantum yield than the hemicage complex (see Table 1), accounting for the observed decrease in emission intensity with irradiation. Evidently, ligand loss does occur, but the resulting species (in which two bpy groups of the hexadentate ligand are coordinated and the third, photodissociated bpy is dangling but still attached via the capping group) can either self-anneal to reform the hemicage complex or combine with a similar complex to form a dimer. The quantum yield for dimerization was determined to be 7.4×10^{-6}. This low value is consistent with the high energy of activation for crossover to the dd excited state, from which ligand dissociation leading to dimer formation must arise. However, since the dd state is still a factor, the photoinertness must be at least partially due to the ability of the complex to undergo reannealing. The superior resistance to ligand photodissociation demonstrated for this complex makes it an excellent candidate for use as a sensitizer for light to chemical energy conversion.

The quenching behavior of $[Ru(5\text{-bpy-}2C)_3Bz]^{2+}$ was also investigated with a selection of quenchers including oxygen and $[Fe(phen)_3]^{2+}$, energy-transfer quenchers; methyl viologen, an electron acceptor; and two electron donor quenchers, phenothiazine and 4-aminoveratrole. Stern−Volmer plots were prepared, and quenching rate constants, k_q, were calculated for $[Ru(5\text{-bpy-}2C)_3Bz]^{2+}$ and its parent complex, $[Ru(5,5'\text{-dmb})_3]^{2+}$. Results are summarized in Table 4. With all quenchers except oxygen, the hemicage complex gave somewhat larger quenching constants than the parent complex. In the case of methyl viologen, the difference is probably insignificant, as these k_q values are within experimental error.

The most dramatic increases in k_q for the hemicage complex were noted for the reductive quenchers. Previous studies revealed that the $Ru^{II/I}$ couple is 30 mV less negative for the hemicage complex than for the parent complex.[14] The increased driving force for electron transfer undoubtedly contributes to the elevated k_q values for $[Ru(5\text{-bpy-}2C)_3Bz]^{2+}$, however it is unlikely that this effect alone can explain the observed increase (by more than a factor of 2) in k_q with the quenchers,

(33) Caspar, J. V.; Meyer, T. J. *J. Am. Chem. Soc.* **1983**, *105*, 5583.
(34) Allen, G. H.; White, R. P.; Rillema, D. P.; Meyer, T. J. *J. Am. Chem. Soc.* **1984**, *106*, 2613.

phenothiazine and 4-aminoveratrole. Perhaps there are forces of attraction between the hydrophobic capping group on the hemicage complex and the aromatic quencher molecules that keep these species in closer proximity, allowing more frequent encounters which result in reductive quenching.

The quenching rate constants for the hemicage and parent complexes with oxygen are within experimental error and are near the diffusion limit. Based on this result, it can be concluded that the capping group on the hemicage complex does not shield the chromophore from bimolecular interactions with small molecules. Because of its long lifetime and high k_q, $[Ru(5\text{-bpy-}2C)_3Bz]^{2+}$ is well suited for use as a quenchometric oxygen sensor. The lifetime varies from 25 ns in oxygen saturated acetonitrile (8.1 mM at 25 °C) to more than 100 times that value in nitrogen-sparged solution.

Conclusions

The three hemicage ruthenium(II) complexes, $[Ru(5\text{-bpy-}2C)_3Bz]^{2+}$, $[Ru(4\text{-bpy-}2C\text{-}Ph)_3Et]^{2+}$, and $[Ru(4\text{-phen-}2C\text{-}Ph)_3Et]^{2+}$ prepared from podand-type ligands, **1**, **2**, and **3**, exhibited longer excited-state lifetimes and higher emission quantum yields than the corresponding model complexes, $[Ru(5,5'\text{-dmb})_3]^{2+}$, $[Ru(4,4'\text{-dmb})_3]^{2+}$, and $[Ru(4\text{-Mephen})_3]^{2+}$. These enhanced photophysical properties can be partially attributed to a decrease in the rate of nonradiative decay via vibrational deactivation which accompanies the increase in rigidity of the complexes. Of the three hemicage complexes, the longest lifetime was observed for the tris(phenanthroline) chromophore, despite the fact that its parent complex is the shortest-lived of the three. This is most likely a consequence of the decreased role of the dd state in the deactivation of hemicage complexes. A comparison of the two bipyridine complexes showed that the more rigid of the two structures has the longer lifetime and higher emission quantum yield.

In the case of $[Ru(5\text{-bpy-}2C)_3Bz]^{2+}$, it was demonstrated that the activation energy for crossover to the dd state is considerably higher than for $[Ru(bpy)_3]^{2+}$, despite the fact that the hemicage structure does not significantly perturb the first coordination sphere and has little effect on the ground state properties of the chromophore. The decreased accessibility of the dd state plays an important role in the enhanced lifetime of the hemicage species as well as being responsible for the decreased rate of photoinduced ligand loss chemistry. The only photoproduct observed upon long-term irradiation of $[Ru(5\text{-bpy-}2C)_3Bz]^{2+}$ appears to be a dimer species, $[Ru_2((5\text{-bpy-}2C)_3Bz)_2]^{4+}$. No evidence for the formation of dichloro- or disolvato- complexes was observed, possibly due to the fact that a photodissociated bipyridine ligand is held tethered to the complex such that it can be recoordinated.

The hemicage complexes reported here, especially $[Ru(5\text{-bpy-}2C)_3Bz]^{2+}$, are excellent candidates for use as photosensitizers for a variety of applications. The long lifetime, high emission quantum yield, and superior photoinertness have been achieved without affecting the useful photoinduced electron-transfer and energy-transfer capabilities of the chromophore. Future work to construct modified hemicage complexes which can be used as building blocks for the construction of molecular assemblies is planned.

Acknowledgment. We thank the donors of the Petroleum Research Fund, administered by the American Chemical Society, for financial support of this work. Additional undergraduate student stipends were provided by Davidson College. NMR studies at Davidson College were conducted on an instrument acquired through an NSF ILI grant. Acknowledgment is made to the Scripps Research Institute for use of mass spectrometers and to the University of North Carolina at Chapel Hill and James Madison University for access to instruments for photochemical and photophysical measurements. We also thank John Moss and Durwin Striplin for their assistance with the temperature-dependent lifetime study and for helpful discussion.

Supporting Information Available: Figures showing the ^1H NMR spectrum of $[Fe(5\text{-bpy-}2C)_3Bz](PF_6)_2$ in CD_3CN (aromatic and methylene regions); ESI mass spectrum of Ru(II) complex with L = (4-bpy-2C-Ph)$_3$Et, BAND B1 (low-resolution spectrum as well as high-resolution spectrum of RuL^{2+} peak); ESI mass spectrum of Ru(II) complex with L = (4-phen-2C-Ph)$_3$Et, BAND C1 (low-resolution spectrum as well as high-resolution spectrum of RuL^{2+} and $RuL(PF_6)^+$ peaks) are available (4 pages). Ordering information is given on any current masthead page.

IC971322F